This is the author version of an article published as:

Keen, Imelda and Raggatt, Liza and Cool, Simon and Nurcombe, Victor and Fredericks, Peter M. and Trau, Matt and Grondahl, Lisbeth (2007) Surface Roughness and Topography of Poly(3-hydroxybutyrate-co-3-hydroxyvalerate) Influences Osteoblast Cell Growth. *Journal of Biomaterials Science, Polymer Edition* 18(9):pp. 1101-1123.

Surface Roughness and Topography of Poly(3-hydroxybutyrate-*co*-3-hydroxyvalerate) Influences Osteoblast Cell Growth

Imelda Keen[1,#], Liza J. Raggatt[2,#], Simon M. Cool[4,5], Victor Nurcombe[4], Peter Fredericks[6], Matt Trau[1] and Lisbeth Grøndahl[3,*]

[1]Nanotechnology and Biomaterials Centre, [2]Institute for Molecular Bioscience, [3]School of Molecular and Microbial Sciences, The University of Queensland, Brisbane, Queensland, 4072 Australia

[4]Institute of Molecular and Cell Biology, 61 Biopolis Drive, Singapore 138673

[5]Department of Orthopaedic Surgery, National University of Singapore, Singapore 117597

[6]School of Physical and Chemical Sciences, Queensland University of Technology, Brisbane, Queensland, Australia

[#]I.K and L.J.R contributed equally to this study

Abstract

Osteoblast proliferation is sensitive to the topography of material surfaces. In this study, the proliferation of MC3T3 E1-S14 osteoblast cells on poly(3-hydroxybutyrate-*co*-3-hydroxyvalerate) (PHBV) films with different surface characteristics was investigated. The solvent cast films were prepared using three different solvents/solvent mixtures; chloroform, DCM and a mixture of chloroform and acetone which produced PHBV films with both a rough (at the air interface) and smooth (at the glass interface) surface. Investigation of the surface characteristics by scanning electron and scanning probe microscopies revealed different surface topographies and degrees of surface roughness ranging from 20 to 200 nm. Mapping of the surface crystallinity index by micro-attenuated total reflectance Fourier transform infrared (ATR-FTIR) showed distinct variations in surface crystallinity between the different film surfaces. Water contact angles were significantly higher on the rough surface compared the smooth surface for a particular substrate, however, all surfaces were hydrophobic in nature (θ_A was in the range 69 - 80º). MC3T3 E1-S14 osteoblast cells were cultured on the six different surfaces and proliferation was determined. After 2 days cell proliferation on all surfaces was significantly less than on the control substrate, however, after 4 days cell proliferation was optimal on the three surfaces that displayed the highest contact angle and the smallest crystallinity heterogeneity. In addition, the surface roughness and more specifically the surface topography influenced the proliferation of osteoblast cells on the PHBV film surface.

Keywords: surface topography; surface roughness; surface crystallinity; wettability; PHBV; MC3T3 E1-S14 cells; osteoblast proliferation

Introduction

Artificial bone scaffolds that have properties akin to native bone and that can be made on demand and shaped as required during surgery would be a valuable recourse for orthopaedic surgery [1-4]. Current options available to replace bone include allograph and autograph bone, however, there is a limit to the amount of autograph bone that can be harvested, and allograph bone must be irradiated before it can be used, a process which severely compromises the quality of the bone. Thus, the fabrication of artificial bone scaffolds that can be used to replace and repair injured or diseased bone is a clinical necessity that can be achieved by using biodegradable polymers [1-4].

The biodegradable polymer poly(3-hydroxybutyrate-*co*-3-hydroxyvalerate) (PHBV) which is derived form various micro-organisms, including the energy storage granules of gram negative bacteria, has a number of intrinsic features suitable for making an artificial bone biomaterial. Specifically, PHBV has a slow degradation rate which allows sufficient time for the bone to repair itself and it forms degradation products which are non-toxic and which are metabolized through beta oxidation and the tricarboxylic acid cycle (TCA cycle) [2-4]. In addition, PHBV has mechanical properties which are superior to those of cancellous bone (Young's modulus of 1.0 GPa and tensile strength of 13 MPa) [5] and which can be improved further by the generation of composite biomaterials made from PHBV and hydroxyapatite [6, 7]. Recent studies have shown that PHBV supports the growth and proliferation of osteoblast cells [8, 9]. However, it appears that the growth and differentiation of osteoblast cells on PHBV is affected by a lag period [9] and surface roughness and wettability of the PHBV substrate are the properties proposed to hinder the initial grow of osteoblast cells on PHBV [9]. Other studies have shown that the proliferation

and differentiation of osteoblast cells on biomaterial substrates is affected by the unique surface properties of the particular material used. Specifically, surface wettability, [10] roughness, [11, 12] crystalinity [13] and topography [14] have been shown to influence the behaviour of osteoblast cells grown on polymer based biomaterials.

Low surface wettability (i.e. high hydrophobicity) is a common surface characteristic of many polyesters including PHBV. Hydrophobicity reflects the surface energy of a substrate and influences the adsorption of proteins onto materials surfaces [15, 16] and this is know to influence directly the behaviour of cells grown on the substrate [10]. Specifically, hydrophobic surfaces (polystyrene bacteriological culture plastic, water contact angle 75°) are known to inhibit proliferation and increase the rate of apoptosis of anchorage-dependent osteoblastic cells compared to cells grown on hydrophilic surfaces (tissue culture grade polystyrene, water contact angle 56°) [10].

Surface roughness (R_a) has been investigated extensively and been shown to influence osteoblast proliferation on several polymer substrates [11, 12]. Wan *et al* generated patterned polymer surfaces and demonstrated that both micro- (2.5 μm) and nano- (40 nm) scale poly(L-lactide) (PLLA) islands, and polystyrene (PS) pits, improved the attachment of rat osteoblast-like cells to both materials. Hatano *et al.* have also demonstrated the role of surface roughness in promoting the osteoblastic proliferation of rat calvarial osteoblastic cells by changing the roughness (37nm to 2.9 μm) of PS surfaces with different coarseness of grinding paper [11]. Patterned surfaces have also been used to investigate important surface parameters other than R_a as lateral distribution of the topography features has been suggested to be a crucial factor for

determining cell response [13]. Liao *et al.* found that rat calvaria bone cells preferred pyramid patterned silicone surfaces (square base 33 μm, height 23 μm) compared to flat featureless surfaces [14] and proposed that the grooves between the patterned surface features created a specific biochemical micro-environment around each cell which promoted proliferation [14]. In addition to the alignment of the surface pattern influencing cell behaviour, the sizes of the topographical features (grooves or pits) are also influential and can limit the interaction of rat calvaria bone cells with the surface as cell filopodia have been observed to anchor on top of a surface feature rather than on the surface in between them [17].

Annealing can modify the degree of polymer crystallinity which can also affect surface topography [13]. By limiting the time of the crystallisation process Washburn *et al*. produced PLLA films with differing degrees of crystallinity and surface roughness on the nano scale (1-10 nm) [13]. The rate of proliferation of MC3T3-E1 osteoblastic cells was found to be greater on the smooth regions of the films than on the rougher regions, however, as the changes in surface crystallinity were not assessed in this study it is not possible to definitively identify which surface parameter, roughness or cystallinity, was the most influential.

While the generation of patterned polymer surfaces can provide important information regarding cellular responses to surface topography on biomaterial films, these fabrication techniques are not transferable and can not be applied to the generation of surface features within 3D scaffolds. Solvent casting, however, is a technique that can be used to create a variety of surface features on polymer films and in addition, this procedure somewhat mimics the process occurring in solvent based 3D scaffold

production. Polymers with differing degrees of crystallinity, wettability and topography can be produced by using different solvents during solvent casting [18-20] and the surface characteristics of these solvent cast films can also be influenced by the type of casting substrates [21, 22].

The identification of the optimal surface properties of PHBV to support osteoblast growth and differentiation is essential given the promise this polymer has as an artificial bone substrate. The aim of this study was to identify the optimal surface features of solvent cast PHBV required to support osteoblast proliferation. Solvent cast films were produced in this study from a variety of solvents. Surface characteristics of the different films were determined using scanning probe microscopy (SPM), scanning electron microscopy (SEM), attenuated total reflectance Fourier transform infrared (ATR-FTIR) spectroscopy and contact angle measurements. The differences in surface properties were then correlated to the proliferation of osteoblast cells cultured on the different films.

Materials and Methods

Preparation of solvent cast films

Poly(3-hydroxybutyrate-*co*-3-hydroxyvalerate) (PHBV) with 8.8 mole% of 3-hydroxyvalerate was purchased from Sigma-Aldrich (St. Louis, USA). Films were produced by dissolving at 50°C approximately 0.30 g of PHBV in 15 ml of solvent; either chloroform (99.4% purity, Proanalys), dichloromethane (99.8% purity, Labscan), or a chloroform/acetone (99.5% purity, Ajax) (50/50 v/v %) mixture. When the chloroform/acetone solvent mixture was used, the powder was dissolved first in chloroform before acetone was added. A covered glass Petri dish (70 mm i.d.) was used as casting substrate. Solvents were allowed to evaporate at room temperature (25ºC) over several days. Two types of surfaces resulted; a 'rough' surface was produced at the air interface and a 'smooth' surface was produced at the glass interface. Sample surfaces were labelled as follows: $CHCl_3$-R; rough surface of the chloroform cast PHBV film, $CHCl_3$-S; smooth surface of the chloroform cast PHBV film, DCM-R; rough surface of the DCM cast PHBV film, DCM-S; smooth surface of the DCM cast PHBV film, MIX-R; rough surface of the chloroform/acetone cast PHBV film, and MIX-S; smooth surface of the chloroform/acetone cast PHBV film.

Characterisation of solvent cast films

Scanning Electron Microscopy (SEM)

Samples were secured on aluminium stubs using carbon double sided tape and then sputter coated with platinum (Eiko, Japan) to prevent the sample from charging during image acquisition. SEM images were obtained using a JEOL-6400F scanning electron microscope at an accelerating voltage of 5 to 10 kV. Digital images were captured and saved using an image slaver software program.

Scanning Probe Microscopy (SPM)

An NT-MDT Solver P47 SPM (NT-MDT Co., Russia) was used in a semi-contact ("tapping") mode to obtain information on surface roughness of the samples. Measurements were done using non-contact “Golden” Si cantilevers (type NSG11 from NT-MDT Co, Russia) with a nominal tip radius of about 10 nm and a scan speed of approximately 1 Hz. The cantilever had a force constant of 5 N/m. Scans were done over a nominal area of either 7.5 μm × 7.5 μm or 18.0 μm × 18.0 μm. A minimum of four areas on each surface were scanned.

Contact Angle Measurements

Water contact angle measurements were acquired using the sessile drop method [23]. Both advancing (θ_A) and receding (θ_R) contact angles were obtained by delivering drops of Milli-Q water on the film surfaces with a minimum of three repeats for each sample. The advancing (θ_A) contact angle was measured on a 5 μL drop and subsequently after each addition of 5 μL until a total 20 μL volume was added. For receding (θ_R) contact angle, a 5 μL increment was withdrawn from a 25 μL water drop for each contact angle measurement. Using the equation $2h / \Delta = \tan \theta / 2$, contact angles ($\theta$) were calculated ($\Delta$ is the base diameter of the drop and h is the height of the drop) [23].

Attenuated Total Reflectance Fourier Transform Infrared (*ATR-FTIR) Spectroscopy*

ATR-FTIR spectra (64 scans, 8 cm^{-1} resolution, wavenumber range 4000-525 cm^{-1}) were acquired using a Nicolet Nexus 870 (Thermo-Nicolet, Madison, WI, USA) with a Smart Endurance diamond ATR accessory where the penetration depth was 0.91 μm

at 1550 cm^{-1} when using a value of 1.5 for the refractive index of the polymer. Micro ATR-FTIR spectra (64 scans, 8 cm^{-1} resolution, wavenumber range 4000-700 cm^{-1}) were collected from a Nicolet Continμum microscope equipped with a liquid nitrogen cooled mercury-cadmium-telluride (MCT) detector and a silicon ATR objective attachment where the penetration depth was 0.65 μm at 1550 cm^{-1}. Contact between the crystal and sample was automated and monitored by a pressure gauge. An area of 1000 μm × 1000 μm was mapped where each spectrum was obtained from an area defined by an aperture of 40 μm × 40 μm. ATR spectra were corrected for wavelength dependence. The step size for each spectrum was 40 μm. Spectral information was extracted by means of spectral analysis software (GRAMS/32, Galactic Industries Corp., Salem, NH) and maps were illustrated using the Origin graphics software package (OriginLab Corp.).

X-ray Diffraction (XRD) Spectroscopy

XRD spectra were recorded on a Bruker D8 Advance X-Ray diffractometer equipped with Cu Kα (λ =0.1542 nm) source and Göbel mirrors to achieve a parallel X-ray beam. Each scan was recorded in the range of 2θ = 6-36° at a scan step of 0.01°/10 s at 40 kV and 30mA. Traces were processed using the Diffrac^{plus} Evaluation Package Release 2004 and PDF (Powder Diffraction File)-2 Release 2004. Percent crystallinity was calculated from the crystalline and total area of the diffractogram and carried out using Peak Fit Version 5 and Excel software.

Differential Scanning Calorimetry (DSC)

A Perkin Elmer DSC 7 was calibrated using the melting temperatures of indium (429.4 K) and zinc (692.5K) and their heats of fusion. About 5 mg specimens were

heated from 20 ºC to 200 ºC at a rate of 10 ºC/min. Melting enthalpy (ΔH_m) was determined from the area under a peak of the DSC trace run using a data acquisition program (PYRIS Version 3.5 Thermal software). Percent bulk crystallinity was determined by using the following equation:

$$\% \text{ bulk crystallinity} = (\Delta H_m)/(\Delta H_m^*) \times 100\%$$

where ΔH_m^*, the enthalpy of fusion for 100% crystalline PHB, was taken to be equal to 146 J/g [24].

Osteoblast Cell Studies

Cell Morphology Assessment and Cell proliferation Assay

Cell morphology and proliferation assays involved culturing MC3T3-E1-S14 (MC3T3) cells on tissue culture plastic, PHBV or glass substrates for 2 and 4 days. The MC3T3 cells were grown in Minimal Essential Media (Invitrogen) supplemented with 10% fetal bovine serum (Invitrogen), 50 units/ml penicillin G sodium, 50 μg/ml of streptomycin sulfate and 2 mM L-Glutamax. To ensure that the cells only adhered to the glass or PHBV substrates and did not migrate onto the tissue culture plastic wells into which the glass and PHBV substrates were placed; the tissue culture plastic wells were pre-coated with 30 μl/cm^2 of 12% poly(2-hyroxyethylmethacrylate) in 95% Ethanol (Sigma, St Louis, USA). The poly(2-hyroxyethylmethacrylate) was allowed to harden overnight, the different PHBV substrates were placed into wells and the MC3T3 cells were seeded the following day at 2x10^3 cells/well in a 96 well plate and grown for 2 and 4 days at 37 °C in 5% CO_2.

To assess cell morphology at the end of the culture period, the cells were incubated for 30 min at 37 °C in 4% paraformaldehyde. The cells were then washed 3 times in

de-ionized water, incubated in Harris haematoxylin for 5 min and then washed 3 times in tap water. The PHBV and glass cover slips where then mounted in aqueous mounting media. Cells were visualized and imaged on an Olympus IX-70 microscope using a SPOT RT camera and SPOT^{TM} 3.2.6 software.

Cell proliferation was assessed indirectly using the CellTiter® 96 Aqueous One Solution Cell Proliferation Assay, a methylthiazol tetrazolium (MTT) assay (Promega, Madison, USA), which measures the activity of the subcellular mitochondrial enzyme succinate dehydrogenase spectrophotometrically. At the end of the culture period a final concentration of 200 μg/ml of MTT solution was added to all wells and the cells were incubated for a further 2 h at 37 °C in 5% CO_2 before being read on a Powerwave XS spectrophotometer using KCjunior software (Bio-TEK instruments) at 490nm using a reference wavelength of 600nm.

To assess the effect of conditioned media, solvent and lipopolysaccharide (LPS) on MC3T3 cell viability, the cells were cultured on tissue culture plastic and treated with these respective agents. Cells were allowed to adhere and then treated for 2 or 4 days with media that had been conditioned by soaking in either, $CHCl_3$, DCM or MIX cast PHBV for either 2 or 4 days. For LPS and solvent treatment, the cells were treated with 0.01-10 ng/ml of LPS or 1 - 0.0001% of the respective solvents from the time of cell seeding for either 2 or 4 days, and cell viability was then assessed using the MTT assay described above.

Statistical analysis

Statistically significant differences in the proliferation assays were determined by one way analysis of variance (ANOVA) followed by a Tukey's Multiple Comparison Test using the GraphPad software program PRISM.

Results

Topography

Chloroform and a mixture of chloroform/acetone solvents have been used previously to change the surface features of biodegradable polymers other than PHBV [20]. In the current study, DCM was used in addition to these two solvent systems. SEM images obtained for PHBV films from the rough side (air interface) and the smooth side (glass interface) of each of the solvent cast films are shown in Figure 1. Comparing the SEM micrographs of the rough side of each of the films reveals different morphological patterns. The $CHCl_3$-R surface has pits of 2-5 μm in diameter and up to 2 μm apart; while the DCM-R surface has pits of 1-2 μm which are up to 3 μm apart. Distinctly different surface features comprising larger pits in the range of 5-20 μm, with ridges in between of up to 8 μm in width were obtained when a mixture of chloroform and acetone was used to produce the PHBV film (i.e. MIX-R). The smooth side of the different films reveal a more uniform surface topography compared to the rough side. However, there are some differences between the smooth sides with the MIX-S surface appearing to have the most featureless surface similar to that found previously for melt processed PHBV [25].

Surface Roughness

Surface roughness was assessed using SPM. R_a values (the mean value of surface roughness relative to the centre plane) and R_z values (the maximum height between pits and groves) are listed in Table 1. The rough surfaces of all three films displayed relatively high R_a values (150 – 210 nm) which were not significantly different. The smooth surfaces were all significantly different (both to the rough surfaces and between the different smooth surfaces) with the MIX-S surface displaying the

smallest R_a value (20 ± 10 nm). R_z values were found to parallel the R_a values, but displayed less discrimination between the smooth surfaces.

Surface Hydrophobicity

Contact angle values of the different PHBV film surfaces are tabulated in Table 1. There was no significant difference between the advancing contact angles of the rough side compared to the smooth side of each of the films, apart from a tendency for the rough side to have a slightly higher advancing contact angle. The advancing contact angles for the $CHCl_3$-R and DCM-R surfaces were similar but 10° higher than the MIX-R surface. The smooth side of the films followed a similar trend with the $CHCl_3$-S and DCM-S surfaces having higher advancing contact angles than the MIX-S surface. Contact angle hysteresis ($\theta_A - \theta_R$) was low for all samples and the surfaces with the lowest roughness values (DCM-S and MIX-S) did display the lowest hysteresis as expected.

Bulk Crystallinity

The bulk crystallinity of the PHBV powder as received was found by X-ray diffraction (XRD) to be 51%. The bulk crystallinity for each of the three films of this study fell within the range of 35-38% and was not significantly different for the three films (Table 1). In general, samples with differing crystallinity are measured to obtain intrinsic values to be utilised for the calculation of percent crystallinity by indirect methods such as DSC and vibrational spectroscopy [26-28]. In the current study, the crystallinity calculated from the DSC measurement agreed with that obtained by XRD for each sample when the value of 146 J/g for the enthalpy of fusion for 100% crystalline PHB was used [24].

Changes in infrared band intensity, band shape or position during heating can reveal bands in the infrared spectra that are sensitive to a change in crystallinity [26-28]. Bloembergen *et al* observed from the infrared spectrum of PHBV that the intensity of the band at 1185 cm^{-1} displayed the largest difference between crystalline and amorphous states. A crystallinity index, CI, was determined by normalising the 1185 cm^{-1} band to that of the 1382 cm^{-1} band, which was found to be insensitive to the degree of crystallinity [28]. The CI is a relative measure of crystallinity and can be used to compare crystallinity between different samples. Figure 2 shows two infrared spectra from PHBV samples of different crystallinity obtained using a diamond ATR accessory. The band at 1382 cm^{-1} is similar in shape and intensity, however, the band at 1185 cm^{-1} showed different intensity in the two spectra. When the absorbance intensity of the 1382 cm^{-1} band was divided by that of the 1185 cm^{-1} band the top spectrum exhibited a lower CI value compared to the bottom spectrum. PHBV powder as received yielded a CI value of 1.21 while a solvent cast $CHCl_3$ film yielded a CI value of 0.96. Comparing these values with the absolute crystallinity obtained by XRD it can be seen that a higher CI value corresponds to a higher crystallinity, thus, verifying the use of the CI values to assess relative magnitudes of crystallinity.

Surface Crystallinity

Typically, infrared spectral data are collected from a large volume of a sample. This procedure yields information about the whole area of analysis (i.e. surface and bulk) and does not provide the spatial distribution of crystalline and non-crystalline domains within a surface. The fraction and location of crystalline and non-crystalline domains within a polymer is affected by the processing method [13, 18-20]. By

acquiring an infrared map by the point illumination method using an ATR objective, heterogeneous surfaces can be explored. The micro ATR-FTIR technique probes the surface (see methods section) using evanescent infrared light [29] and can be used to map a surface by building up a mosaic of infrared spectra recorded at discrete points in a grid pattern. This allows for the determination of the distribution of components across a sample surface [30]. Figure 3A show such a micro ATR-FTIR map where the distribution of CI values can be seen on the DCM-S surface. In the CI gradient the red colouration indicates the highest CI values. For the DCM-S surface, a CI range (difference between the highest and the lowest CI value) of 0.60 was measured (Table 1). The CI map of the $CHCl_3$-R surface showed a significantly smaller CI range, thus presenting a less heterogeneous surface (Figure 3B). In addition, this surface is less crystalline than the DCM-S surface as assessed by the absolute CI values. Surface CI maps of all surfaces were obtained and their CI range values are tabulated in Table 1. The DCM-S surface showed the highest CI value (i.e. 1.60) and largest CI range while the $CHCl_3$-S surface showed the lowest surface CI value (i.e. 0.70).

Osteoblast Cell Morphology

To investigate the influence of the PHBV material surface properties on the morphology of osteoblast cells, *in vitro* culture of MC3T3 cells on the different PHBV substrates was performed for 4 days, after which the cells were fixed and stained with hematoxylin (Figure 4). On the $CHCl_3$-R, $CHCl_3$-S, the DCM-R and the MIX-S surfaces the morphology of the cells was the same as that seen for cells grown on glass. The cells were flat and spread on these surfaces. However, the morphology of the cells grown on the DCM-S and the MIX-R surfaces was different to that of cells grown on glass. The cells were less spread and exhibited a large number of

processes extending on to the DCM-S and the MIX-R materials. There was also a striking reduction in the number of cells seen on the MIX-R surface compared to all the other substrates tested, suggesting that the proliferation of cells was significantly influenced by the different PHBV substrates (Figure 4).

Osteoblast Cell proliferation

To identify differences in the proliferation of osteoblast cells grown on the different PHBV substrates an indirect assessment of proliferation was used. A MTT assay was performed on cells grown on different PHBV substrates to directly measure the metabolic rate of the cells. As the metabolic rate the MC3T3 cells is consistent, regardless of the growth substrate, a change in metabolic activity refects a change in the number of cells present and hence the proliferation of cells over time on the different PHBV substrates. There was significantly less proliferation of osteoblast cells grown on all PHBV substrates at day 2 compared to the cells grown on glass (Figure 5A). For some substrates, this lag in cell proliferation was temporary as by day 4 there were no significant differences between the growth of cells seeded on glass, $CHCl_3$-R, $CHCl_3$-S or the DCM-R substrates, indicating that all these substrates can effectively support osteoblast proliferation. However for three of the PHBV substrates, DCM-S, MIX-R and MIX-S, the lag in proliferation persisted as cells grown on these films showed reduced proliferation compared to all other substrates at day 4 (Figure 5B).

Casting of the PHBV films involves the use of solvents that can be toxic to cells and two alternative approaches were taken to eliminate the possibility that the solvent cast films had residual solvent contaminants that were influencing the growth of the

osteoblast cells. Firstly, pieces of PHBV were initially bathed in media prior to the media being added to the cells for the indicated times. Conditioning the media by pre soaking it with different PHBV substrates did not affect proliferation of the osteoblast cells (Table 2). The second approach involved adding the 3 different solvents/solvent mixture to osteoblast cells grown on tissue culture plastic. Only at extremely high concentration of 1% (v/v) of solvent was the proliferation of the osteoblast cells affected (Table 3). Considering that the weight of the PHBV samples used in the cell assays were approximately 2 mg and that no solvent could be detected by FTIR (detection limit estimated to 5%) then the maximum amount of solvent in a PHBV sample would be 0.05 µl. Taking into account that the cell assay used a volume of 200 µl of media, a maximum concentration of solvent produced by elution from the PHBV film would be 0.025%.

PHBV is produced by the fermentation of gram negative bacteria and as such may contain pyrogens such as LPS. Osteoblast cells express the receptor for LPS, Toll-like receptor 4, and LPS has been shown to induce expression of the essential osteoclast regulating cytokine RANKL in osteoblast cells [31]. LPS is also known to influence the proliferation of other cells and thus, to investigate if LPS was influencing the proliferation of osteoblast cells we treated the MC3T3 cells with different concentrations of LPS and assessed their proliferation. No difference in cell proliferation was seen at any of the LPS concentrations investigated (Table 4).

Discussion

Stimulation of bone growth on a biomaterial can be improved by modifying the interface between the biomaterial and its host environment. The material surface properties; roughness, topography, chemistry, crystallinity and wettability, may all affect the biological response that a given material produces. Identification of the specific surface characteristics responsible for influencing cell behaviour is challenging because the modification of one surface property results in simultaneous changes to other surface properties. Hence, the relationship of one particular surface property to cell behaviour is not well understood and needs more rigorous study. Only a few studies on osteoblast cell response to surface properties have thoroughly investigated all the different parameters. In the present study, there is no variation in surface chemistry between samples and all other surface properties have been characterised. This has allowed the surface characteristics (roughness, topography, crystallinity and wettability) to be evaluated for their importance in influencing the growth of osteoblast cells on the biomaterial PHBV.

Formation and nature of surface features

It was found that different surface topographical patterns can be obtained using different solvents for casting PHBV films. The pit patterns produced at the air interphase (the rough surfaces) were produced by water droplets condensing on the surface as the solvent evaporated from the surface of the film [25, 32]. The $CHCl_3$-R and DCM-R surface showed some pits with the diameter sizes being smaller on the DCM-R surface. The size differences of the pit diameters are caused by the different evaporation rate of the solvents. The MIX-R surface has a very different topography pattern compared to the other rough surfaces. During the solvent evaporation process

of this film, it was observed that it gelled after about 2 days and took longer to form a film compared to films made with a single solvent. The surface of the smooth side of the films showed very little texture as the surface characteristics of the casting substrate were retained as an imprint on the polymer surface [22]. In this case, the surface of the glass Petri-dish controlled the topography patterns created on the smooth side.

The roughness (R_a values) obtained for the three rough surfaces, $CHCl_3$-R, DCM-R and MIX-R, are similar within experimental error, however, the surfaces showed vastly different morphological patterns (above). It has been previously pointed out that R_a values do not provide a complete description of the nature of the roughness as it cannot determine any lateral features on the surface [18]. The smooth surfaces all displayed very low R_a values (20-80 nm) with the DCM-S and MIX-S surfaces comparing well with melt processed substrates (R_a = 30 nm) [33] but which are still somewhat rougher than tissue culture plastic (R_a = 6 nm) [9].

All surfaces are hydrophobic in nature with the surfaces produced using the mixed solvents displaying the lowest contact angles. There was a lack of correlation between R_a values and advancing contact angle values, thus, the MIX-R surface displayed one of the lowest advancing contact angles. However, there is a trend for the smooth surface of each set of films to display lower θ_A values than the rough counterparts. The contact angle hysteresis was generally low but no correlation was found between R_a values and contact angle hysteresis, a feature often associated with surface roughness [34].

The CI values obtained for the surfaces studied here were obtained using micro-ATR FTIR. Since different FTIR techniques can result in different CI values it is not possible to compare the results obtained here with those obtained by other groups [28, 35]. Thus the surface CI values can only be used as a comparative measure of crystallinity between the different PHBV surfaces. CI values and ranges of the different surfaces vary significantly between substrates; however, no correlation could be found between CI values and R_a values. However, it is interesting to notice that the group of substrates with the most hydrophobic surfaces ($CHCl_3$-R, $CHCl_3$-S, DCM-R) display the least heterogeneous surface crystallinities (Table 1), although this might be coincidental.

Cell viability on PHBV surfaces

To evaluate appropriately the influence of different PHBV surface properties on the growth of osteoblast cells it was essential to eliminate the possibility that potential surface contaminants were influencing cell proliferation. LPS is a component of gram negative bacterial and as such LPS can be a contaminant of PHBV following its purification from such micro organisms. In addition it is possible that the casting solvents used to produce the PHBV films could leave a residual contaminant on the surface of these substrates and as such this was also investigated. However addition of LPS, the solvents $CHCl_3$, DCM or a mixture of $CHCl_3$ and acetone, or PHBV conditioned media to osteoblast cells had no affect on their proliferation which indicates that the lag in osteoblast proliferation seen with all PHBV surfaces on day 2 (figure 5A) was not due to any contaminating factors but was a consequence of the PHBV substrate.

Surface hydrophobicity is a material property known to influence the growth of osteoblast cells [10]. Specifically it has been reported that hydrophobic surfaces provide a less desirable substrate for cell growth [36, 37]. All the PHBV substrates generated in the current study had water contact angles greater than 65° and as such are classified as hydrophobic, which may account for the lag phase in cell growth that was seen with all PHBV substrates after 2 days. However, it is interesting that by day 4 osteoblast cell proliferation was not different on the two chloroform and the DCM-R surfaces compared to the control surfaces, despite the fact that these were the more hydrophobic PHBV surfaces investigated. This would suggest that as the advancing contact angle values for all the PHBV substrates fell within the hydrophobic classification the 12° of variation between the different PHBV substrates investigated here is not responsible for the differences in osteoblast viability seen after 4 days of growth on these PHBV surfaces.

Surface roughness is another critical parameter that influences cell growth on a given substrate [38, 39]. Many studies have investigated the influence of surface roughness on cell proliferation, however, in the process of altering the roughness of a given substrate, surface chemistry is often changed making it challenging to identify accurately the true effect of roughness alone [40]. Hatano *et al.* have produced an informative study exploring the effect of surface roughness on osteoblast viability. Surface roughness was investigated with minimal changes in surface chemistry by evaluating the effect of different tissue culture plastic roughness on osteoblast proliferation. This study investigated submicron differences in roughness (0.37-2.9 μm) and a roughness of 810 nm was found to be optimal for osteoblast proliferation [11]. The PHBV surfaces generated in the present study also have a surface roughness

in the nanometer to submicrometer range (20-210 nm). The DCM-S and MIX-S substrates generated the smoothest surfaces, with roughness measurements of 20 nm and 40 nm respectively, and it is possible that this property inhibited the proliferation of osteoblast cells on these materials as there was poor proliferation of cells grown on both these materials after 4 days. However, the proliferation results obtained for osteoblast cells grown on the MIX-R surface indicate that roughness is not the only parameter influencing cell behaviour on these PHBV surfaces. Specifically all rough surfaces had the same R_a values within experimental error, however, while the MIX-R substrate was the least effective substrate for growing osteoblast cells of all surfaces tested, the DCM-R and $CHCl_3$-R substrates performed as well as the control surfaces after 4 days, indicating that surface parameters other than the quantifiable classical parameter R_a are influencing cellular growth.

The other surface property that influences cell growth is surface topography which is a more complex description of the surface including both height, the classical descriptive parameter of roughness R_a, as well as size of and distance between topographical features. The differences in osteoblast proliferation on the rough surfaces can not be explained by the hydrophobicity or R_a values and thus appear to be due to a difference in the topographical features of their surfaces. The distance between the surface ridges on the MIX-R surface was 10x greater than the distances on the DCM-R material (5-20 μm and 1-2 μm respectively). The distances between the ridges on the MIX-R surface are approaching the actual size of the MC3T3 cells (30-40um) and it is likely that this inhibits the ability of the cells to spread over these wider valleys and explains the clustering of cells on top of ridged features. This finding is similar to that observed for a study of the interaction of rat calvaria bone

cells with the surface where cell filopodia were observed to anchor on top of a surface feature rather than on the surface in between them [17].

When using polymers as biomaterials it is possible to alter the crystallinity of the surfaces when altering the substrate roughness during the fabrication processing. Washburn *et al.* fabricated poly(L-lactic acid) films with nano scale (0.5-13 nm) differences in surface roughness and found the optimal proliferative response to occur on a surface R_a of 1.1 nm [13]. Interestingly only surface roughness was measured in this study, however as surface crystallinity would also have been altered it is possible that the difference reported in this study were due to changes in crystallinity rather than roughness. In the current study, surface cystallinity was measured and was seen to vary between the different PHBV substrates. Specifically the MIX-R CI values were very similar to those of the MIX-S surface and they both perform poorly with respect to supporting osteoblast growth compared to the control substrates. However, comparing the CI values of the MIX-R substrate (the least capable of supporting osteoblast growth) to that of the $CHCl_3$-R and DCM-R surfaces (which both supported osteoblast growth well) it can be seen that the absolute CI values do not correlate with cellular response. It is, however, interesting to notice that the three substrates which best support cell growth ($CHCl_3$-R, $CHCl_3$-S, DCM-R) have the least heterogeneous surface crystallinity (i.e. smallest CI range). This magnitude in CI range is, however, only slightly different to that of the MIX-S surface and it is therefore unlikely that surface crystallinity is the single most significant parameter influencing cell growth.

Conclusion

Through thorough characterisation of the surface features of solvent cast PHBV films a greater understanding of the parameters which affect osteoblast cell growth on this biomaterial has been obtained. There is no simple correlation between the surface properties of PHBV and the effectiveness of the substrate to support osteoblast proliferation. It is possible that crystallinity heterogeneity contributes to the biological responses reported in this study. However, from the data presented it would appear that for PHBV surface roughness has the greatest influence on osteoblast proliferation. Interestingly, a description of surface roughness that measures the height of surface features does not adequately describe the feature affecting osteoblast proliferation on PHBV with submicron scale roughness, as the spacing of topographical features appears to also be a critical factor influencing osteoblast growth on PHBV.

Acknowledgements

The authors are grateful to the Australian Research Council (Grant No DP0343547) for their support of this project and the National Health and Medical Research Council (Grant ID 252934) for their Peter Doherty Fellowship to Liza Raggatt. The authors would also like to thank the following people for their assistance with data collection and analysis: Ms Anya Yago and Dr Graeme Auchterlonie (Centre for Microanalysis and Microspectroscopy, The University of Queensland) for obtaining the XRD traces and assisting with the calculation of bulk crystallinity, and Dr Thor Bostrom (Analytical Electron Microscopy Facility, Queensland University of Technology, Brisbane) for SPM measurements.

References

[1] Burg KJ, Porter S, Kellam JF. Biomaterial developments for bone tissue engineering. Biomaterials 2000;21(23):2347-59.

[2] Scholz C. Polymers from Renewable Resource: Biopolyesters and Biocatalysis. In: ACS Symposium Series; 2000. p. 328-334.

[3] Gogolewski S, Jovanovic M, Perren SM, Dillon JG, Hughes MK. Tissue response and in vivo degradation of selected polyhydroxyacids: polylactides (PLA), poly(3-hydroxybutyrate) (PHB), and poly(3-hydroxybutyrate-co-3-hydroxyvalerate) (PHB/VA). J Biomed Mater Res 1993;27(9):1135-48.

[4] Taylor MS, Daniels AU, Andriano KP, Heller J. Six bioabsorbable polymers: in vitro acute toxicity of accumulated degradation products. J Appl Biomater 1994;5(2):151-7.

[5] Hammond T, Liggat JJ. Degradable Polymers: Chapman and Hall; 1995.

[6] Doyle C, Tanner ET, Bonfield W. In vitro and in vivo evaluation of polyhydroxybutyrate and polyhydroxybutyrate reinforced with hydroxyapatite. Biomaterials 1991;12(9):841-7.

[7] Lutton C, Read J, Trau M. Nanostructured Biomaterials: a Novel Approach to Artificial Bone Implants. Aust J Chem 2001;54:621-623.

[8] Köse GT, Ber S, Korkusuz F, Hasirci V. Poly(3-hydroxybutyric acid-co-3-hydroxyvaleric acid) based tissue engineering matrices. J Mater Sci Mater Med 2003;14(2):121-6.

[9] Kumarasuriyar A, Jackson RA, Grøndahl L, Trau M, Nurcombe V, Cool SM. Poly(beta-hydroxybutyrate-co-beta-hydroxyvalerate) supports in vitro osteogenesis. Tissue Eng 2005;11(7-8):1281-95.

[10] Chang EJ, Kim HH, Huh JE, Kim IA, Seung Ko J, Chung CP, Kim HM. Low proliferation and high apoptosis of osteoblastic cells on hydrophobic surface are associated with defective Ras signaling. Exp Cell Res 2005;303(1):197-206.

[11] Hatano K, Inoue H, Kojo T, Matsunaga T, Tsujisawa T, Uchiyama C, Uchida Y. Effect of surface roughness on proliferation and alkaline phosphatase expression of rat calvarial cells cultured on polystyrene. Bone 1999;25(4):439-45.

[12] Wan Y, Wang Y, Liu Z, Qu X, Han B, Bei J, Wang S. Adhesion and proliferation of OCT-1 osteoblast-like cells on micro- and nano-scale topography structured poly(L-lactide). Biomaterials 2005;26(21):4453-9.

[13] Washburn NR, Yamada KM, Simon CG, Jr., Kennedy SB, Amis EJ. High-throughput investigation of osteoblast response to polymer crystallinity: influence of nanometer-scale roughness on proliferation. Biomaterials 2004;25(7-8):1215-24.

[14] Liao H, Andersson AS, Sutherland D, Petronis S, Kasemo B, Thomsen P. Response of rat osteoblast-like cells to microstructured model surfaces in vitro. Biomaterials 2003;24(4):649-54.

[15] Ikada Y. Surface modification of polymers for medical applications. Biomaterials 1994;15(10):725-36.

[16] Tamada Y, Ikada Y. Fibroblast growth on polymer surfaces and biosynthesis of collagen. J Biomed Mater Res 1994;28(7):783-9.

[17] Riehle M, Dalby M, Johnstone H, Mackintosh A, Afforssman S. Cell behaviour of rat calvarial cells on the bone surfacs with random nanometric features. Mater. Sci. and Eng. 2003;C23:337-340.

[18] Koegler WS, Griffith LG. Osteoblast response to PLGA tissue engineering scaffolds with PEO modified surface chemistries and demonstration of patterned cell response. Biomaterials 2004;25(14):2819-30.

[19] Kiremitci M, Pulat M, Senvar C, Serbetci AI, Piskin E. Structural and cellular characterization of solvent-casted polyurethane membranes. Clin Mater 1990;6(3):227-37.

[20] Zeng J, Chen X, Xu X, Liang Q, Bian X, Yang L, Jing X. Ultrafine Fibres Electrospun from Biodegradable Polymers. J Appl Polym Sci 2003;89:1085-1092.

[21] Matsuzaka K, Walboomers XF, de Ruijter JE, Jansen JA. The effect of poly-L-lactic acid with parallel surface micro groove on osteoblast-like cells in vitro. Biomaterials 1999;20(14):1293-301.

[22] Smith R, Pitrola R. Influence of Casting Substrate on the Surface Free Energy of Various Polyesters. J Appl Polym Sci 2002;83:997-1008.

[23] Erbil H. Surface Tension of Polymers in Handbook of Surface and Colloid Chemistry. New York: CRC Press; 1997.

[24] Avella M, La Rota G, Martuscelli E, Raimo M, Sadocco P, Elegir G, Riva R. Poly(3-hydroxybutyrate-co-3-hydroxyvalerate) and wheat straw fibre composites: thermal, mechanical properties and biodegradable behaviour. J. Mater Sci. 2000;35:829-836.

[25] Grøndahl L, Chandler-Temple A, Trau M. Polymeric grafting of acrylic acid onto poly(3-hydroxybutyrate-co-3-hydroxyvalerate): surface functionalization for tissue engineering applications. Biomacromolecules 2005;6(4):2197-203.

[26] Runt J. Crystalinity Determination in Encyclopedia of Polymer Scinece and Engineering. New York: Wiley; 1986.

[27] Bower D, Maddams W. The Vibrational Spectroscopy of Polymers. Cambridge: Cambridge University Press; 1993.

[28] Bloembergen S, Holden D, Hmer G, Bluhm T, Marchessault R. Studies of composition and crystalinity of bacteria. Macromolecules 1986;19:2865-2871.

[29] Mirabella F. Internal Reflection Spectroscopy: Theory and Applications. New York: Marcel Dekker; 1993.

[30] Keen I, Rintoul L, Fredericks P. Raman and infrared microspectroscopic mapping of plasma-treated and grafted polymer surfaces. Appl Spectrosc 2001;55:984-991.

[31] Kikuchi T, Matsuguchi T, Tsuboi N, Mitani A, Tanaka S, Matsuoka M, Yamamoto G, Hishikawa T, Noguchi T, Yoshikai Y. Gene expression of osteoclast differentiation factor is induced by lipopolysaccharide in mouse osteoblasts via Toll-like receptors. J Immunol 2001;166(5):3574-9.

[32] Marayuma N, Koito T, Nishida J, Sawadaishi T, Cieren X, Ijiro K, Karthasus O, Shimomura M. Mesoscopic patterns of molecular aggregates on solid substrates. Thin Solid Films 1998;327-329:854-856.

[33] Kenny B. [Honours Thesis]. Brisbane: University of Queensland; 2002.

[34] Kwok D, Neumann A. Contact angle measurment and contact angle interpretaion. Advances in Colloid and Interface Science 1999;81(3):167-249.

[35] Galego N, Rozsa C, Sanshez R, Fung J, Vazquez A, Tomas J. Characterization and application of poly(beta-hydroxyalkanoates) familly as composite biomaterials. Polymer Testing 2000;19:485-492.

[36] Altankov G, Groth T. Fibronectin matrix formation by human fibroblasts on surfaces varying in wettability. J Biomater Sci Polym Ed 1996;8(4):299-310.

[37] Groth T, Altankov G. Studies on cell-biomaterial interaction: role of tyrosine phosphorylation during fibroblast spreading on surfaces varying in wettability. Biomaterials 1996;17(12):1227-34.

[38] Flemming RG, Murphy CJ, Abrams GA, Goodman SL, Nealey PF. Effects of synthetic micro- and nano-structured surfaces on cell behavior. Biomaterials 1999;20(6):573-88.

[39] Anselme K, Bigerelle M, Noel B, Iost A, Hardouin P. Effect of grooved titanium substratum on human osteoblastic cell growth. J Biomed Mater Res 2002;60(4):529-40.

[40] Lincks J, Boyan BD, Blanchard CR, Lohmann CH, Liu Y, Cochran DL, Dean DD, Schwartz Z. Response of MG63 osteoblast-like cells to titanium and titanium alloy is dependent on surface roughness and composition. Biomaterials 1998;19(23):2219-32.

Table 1. Surface properties of PHBV substrates

Sample[a]	R_a (nm)	R_z (nm)	θ_A (º)	$\theta_A - \theta_R$ (º)	CI index (range)	Bulk crystallinity[b]
$CHCl_3$-R	210 ± 40	1700 ± 550	80 ± 3	18 ± 1	0.88 - 1.04 (0.16)	35 %
$CHCl_3$-S	80 ± 10	750 ± 180	79 ± 4	21 ± 1	0.70 – 0.95 (0.25)	
DCM-R	160 ± 40	1300 ± 400	82 ± 4	15 ± 3	0.92 – 1.20 (0.28)	38 %
DCM-S	40 ± 10	350 ± 150	75 ± 2	12 ± 2	0.95 – 1.60 (0.60)	
MIX-R	150 ± 50	1300 ± 550	72 ± 5	13 ± 5	0.80 – 1.20 (0.45)	37 %
MIX-S	20 ± 10	200 ± 70	69 ± 2	12 ± 1	0.80 – 1.15 (0.35)	

a: See Materials and Methods section for an explanation of the acronyms used; b: Determined by XRD

Table 2. Conditioned media from solvent cast PHBV films applied to MC3T3 cells for either 2 or 4 days assayed for proliferation[a].

Days in culture	Chloroform	DCM	MIX Acetone/chloroform
2	93 ± 5	102 ± 2	100 ± 1
4	102 ± 3	107 ± 3	103 ± 2

a: The data is expressed as the average percent in absorbance compared to cells grown in standard media ± standard error of the mean and is representative of three independent experiments.

Table 3. Influence of solvent treatment on the proliferation of MC3T3 cells.

Solvent	% solvent/media (vol/vol)	Cell proliferation[a] 2 days	4 days
Chloroform	1	39 ± 4 [b]	55 ± 1 [b]
	0.1	106 ± 2	99.6 ± 0.7
	0.01	101 ± 4	99 ± 2
	0.001	106 ± 3	98 ± 1
	0.0001	96 ± 2	98 ± 1
DCM	1	59 ± 9 [b]	47 ± 16 [b]
	0.1	104 ± 3	99 ± 3
	0.01	105 ± 3	102 ± 3
	0.001	104 ± 1	99 ± 4
	0.0001	104 ± 1	102 ± 2
MIX	1	27.5 ± 0.2 [b]	25.6 ± 0.3 [b]
	0.1	97.1 ± 0.3	102 ± 2
	0.01	96 ± 2	100.3 ± 0.4
	0.001	94 ± 4	98.7 ± 0.8
	0.0001	98 ± 7	100 ± 3

a: The data is expressed as a percent of untreated cells ± standard error of mean, and is representative of 3 independent experiments

b: Differences between control and treated samples are statistically significant ($p<0.05$).

Table 4. Effect of LPS on MC3T3 cell proliferation.

[LPS] ng/ml	Cell proliferation[a]	
	2 days	4 days
0.01	101 ±7	110 ± 5
0.1	110 ± 4	97 ± 2
1	100 ± 5	99.6 ± 0.5
10	105.1 ± 0.5	98 ± 7

a: The data is expressed as a percent of untreated cells ± standard error of mean and is representative of 3 independent experiments.

Figure captions

Figure 1. Scanning electron microscopy images of the solvent cast PHBV films obtained at 1400X magnification

Figure 2. Micro ATR-FTIR spectra obtained from a $CHCl_3$ cast PHBV film (top spectrum) and PHBV powder as received (bottom spectrum).

Figure 3. Micro ATR-FTIR CI maps obtained from the (A) smooth side of a DCM cast PHBV and (B) rough side of a chloroform cast PHBV films

Figure 4. Morphology of MC3T3 osteoblast cells grown on various substrates for 4 days.
These images are representative of 2 independent experiments. Magnification 10x.

Figure 5. Proliferation of MC3T3 osteoblast cells grown on various substrates; cells grown for 2 (A) or 4 (B) days on the indicated substrates. These data are expressed as average ± standard error of the mean and are representative of 3 independent experiments. * indicates significant differences from cells grown on glass ($p<0.05$).

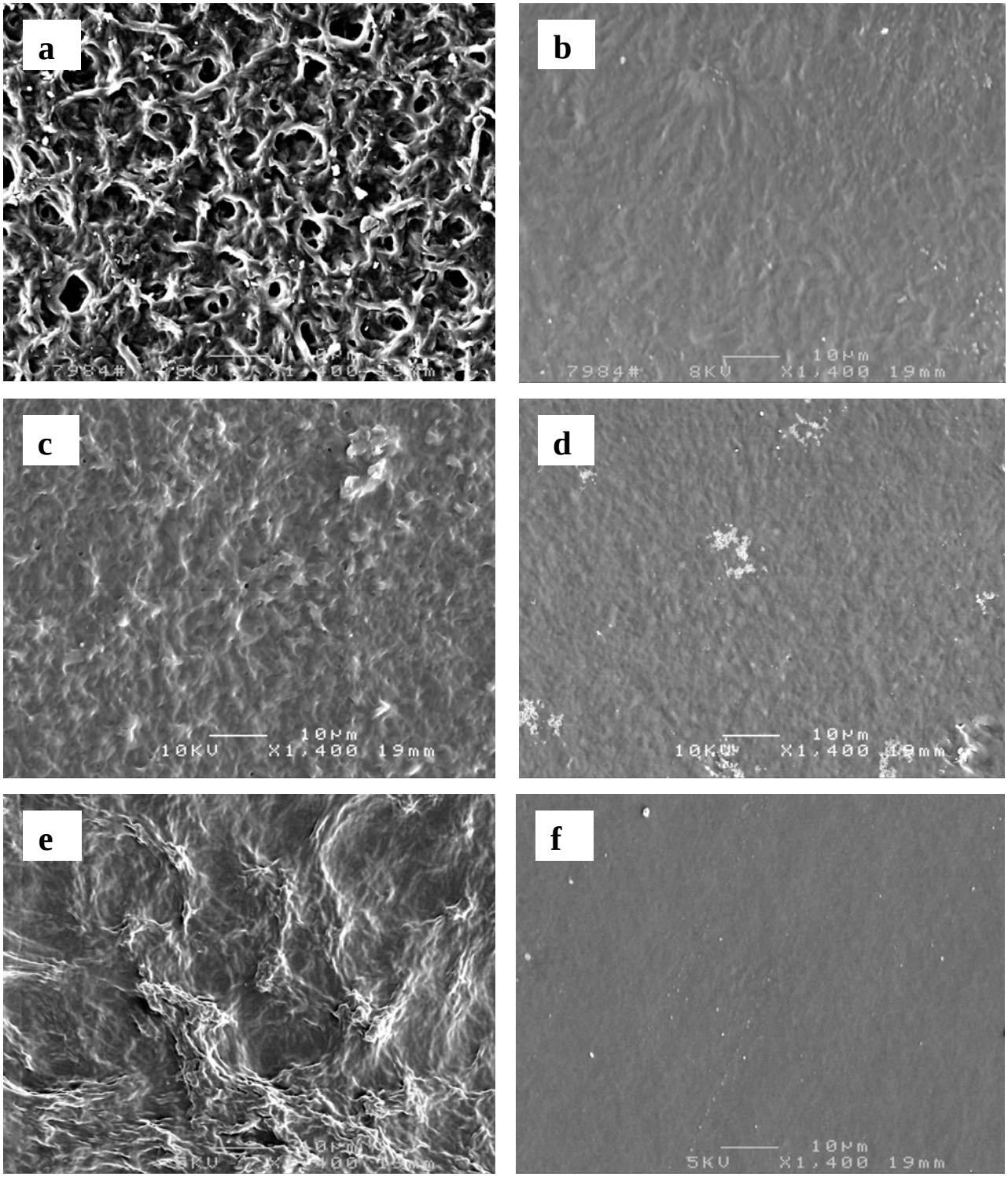
a
b
7984# 8KV X1,400 19mm
10μm
c
10KV X1,400 19mm
d
e
f
5KV X1,400 19mm

Figure 1.

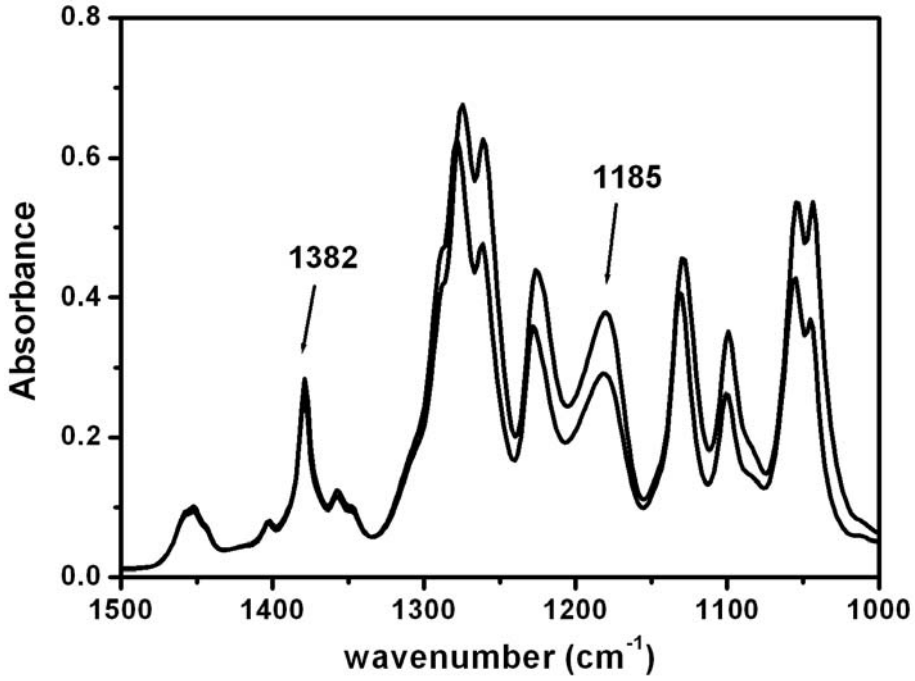
0.8
0.6
0.4
0.2
0.0
Absorbance
1382
1185
1500
1400
1300
1200
1100
1000
wavenumber (cm-1)

Figure 2

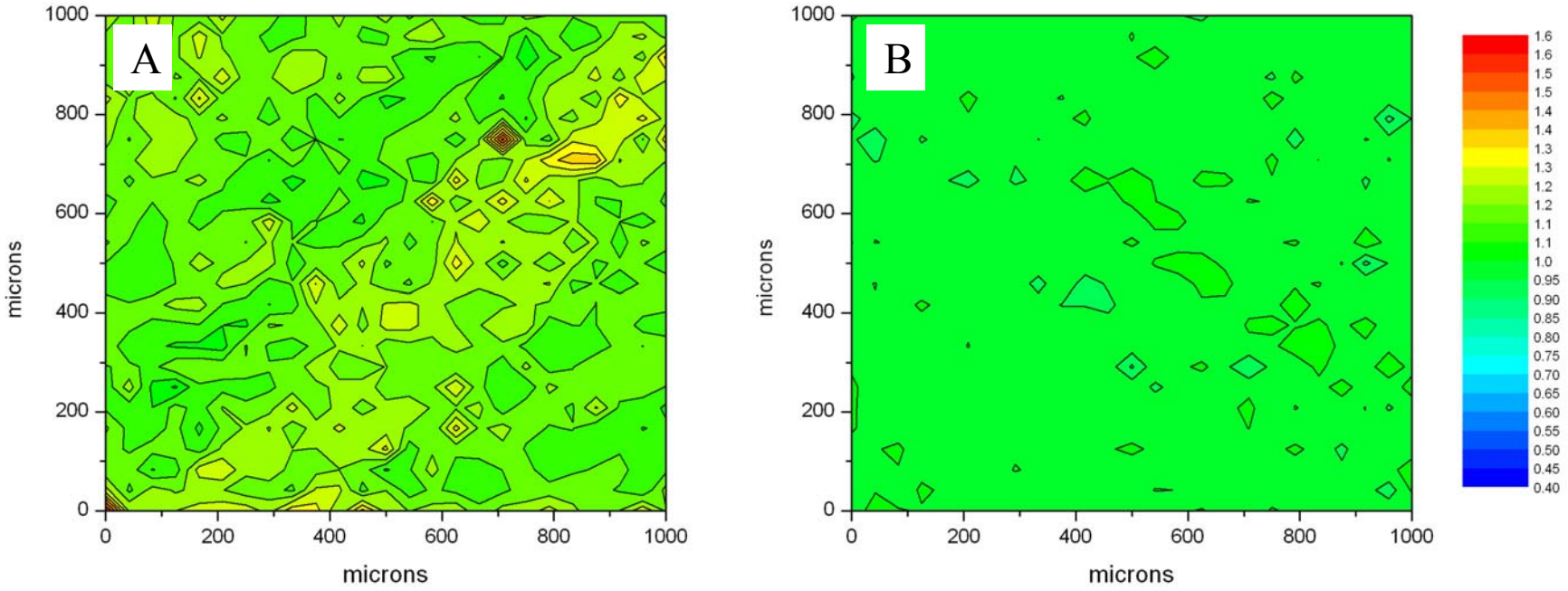
A
B
microns
microns
0
200
400
600
800
1000
1.6
1.6
1.5
1.5
1.4
1.4
1.3
1.3
1.2
1.2
1.1
1.1
1.0
0.95
0.90
0.85
0.80
0.75
0.70
0.65
0.60
0.55
0.50
0.45
0.40

Figure 3.

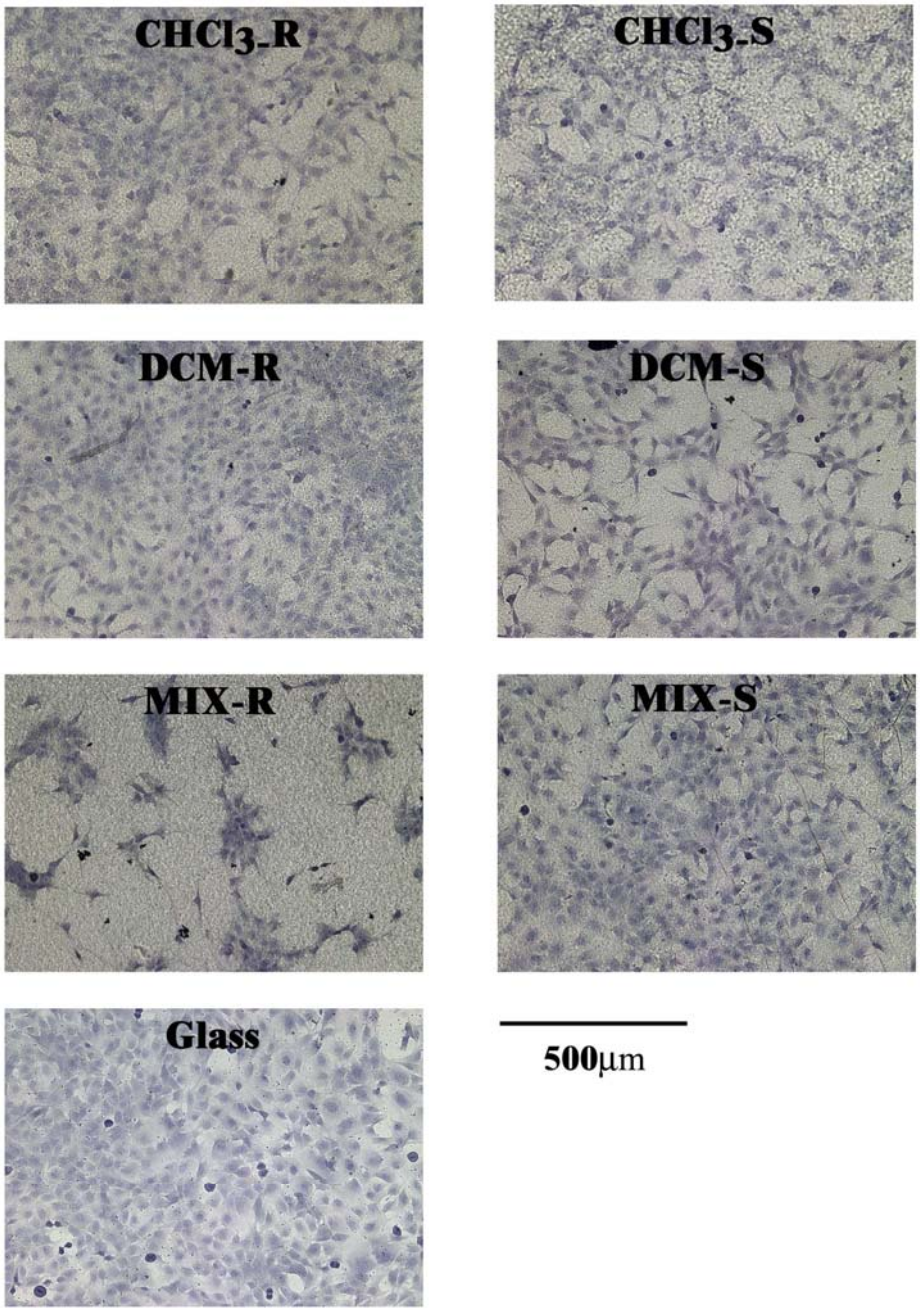

Figure 4.

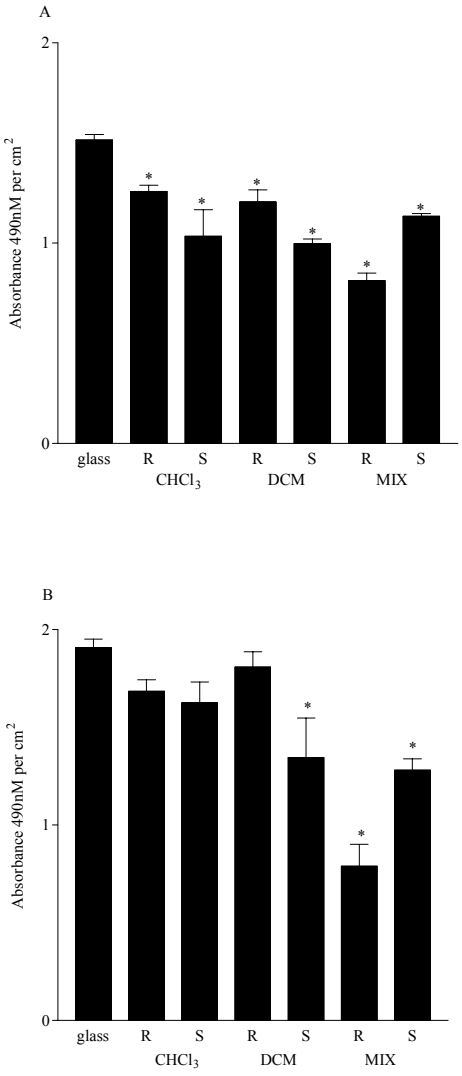
A
Absorbance 490nM per cm2
2
1
0
glass
R
S
R
S
R
S
CHCl3
DCM
MIX
B
Absorbance 490nM per cm2
2
1
0
glass
R
S
R
S
R
S
CHCl3
DCM
MIX

Figure 5.